Journal of Magnetic Resonance 211 (2011) 234–239

Contents lists available at ScienceDirect

Journal of Magnetic Resonance

journal homepage: www.elsevier.com/locate/jmr

Communication

Removal of sidebands in double-rotation NMR in real time

Frédéric A. Perras, David L. Bryce *

Department of Chemistry and Centre for Catalysis Research and Innovation, University of Ottawa, 10 Marie Curie Private, Ottawa, Ontario, Canada K1N 6N5

ARTICLE INFO

Article history:
Received 22 February 2011
Revised 4 May 2011
Available online 15 May 2011

Keywords:
DOR
Sideband suppression
Quadrupolar nuclei
Solid-state NMR
Na-23
DOR sideband simulation
TOSS

ABSTRACT

Double-rotation (DOR) is the only technique generally capable of yielding high-resolution NMR spectra of half-integer quadrupolar nuclei in one dimension for solids without the need for sophisticated coherence pathway selection. Unfortunately, due to the low outer rotor spinning frequencies currently available, the spectra often contain a large number of spinning sidebands which may overlap with the resonances of interest. We implement a simple, robust, and easy to use family of pulse sequences, which in practice are fully analogous to the 'total suppression of sidebands' (TOSS) sequences, to suppress all sidebands arising from the spinning of the outer rotor in DOR experiments. By removing the rotor phase dependence of the evolution of the sidebands, the sidebands destructively interfere with one another during the course of signal averaging to yield 'solution-like' spectra of half-integer quadrupolar nuclei in solids. Advantages and shortcomings of the method compared to other DOR sideband suppression methods are explored with the aid of simulations.

1. Introduction

Nuclear magnetic resonance (NMR) is one of the most important tools for the characterization of chemicals and materials. Since the introduction of magic angle spinning (MAS) [1,2] and cross-polarization [3–5], solid-state NMR of spin-1/2 nuclei such as ^{13}C, ^{31}P, and ^{29}Si has become common practice in materials chemistry. Some of the most important NMR-active nuclei, however, are half-integer spin quadrupolar nuclei such as ^{11}B, ^{17}O, ^{23}Na, and ^{27}Al. These nuclei possess a non-zero electric quadrupole moment that interacts with the electric field gradient (EFG) at the nucleus. The quadrupolar interaction is often too large to be adequately described by first-order perturbation theory [6]. There is thus a large residual broadening in the MAS NMR spectra of such systems that cannot be averaged by conventional means [7].

In double rotation (DOR) NMR, the sample is spun inside a small inner rotor which is itself spun about the magic angle in a larger outer rotor [8,9]. The net motion has the effect of averaging all first and second-order NMR interactions to their isotropic components [10–12]. Unlike multiple-quantum magic-angle-spinning (MQMAS) [13], satellite-transition magic-angle-spinning (STMAS) [14], and dynamic angle spinning (DAS) [15], which typically require a somewhat time-consuming two-dimensional acquisition in order to resolve multiple sites, DOR yields high-resolution ('solution-like') spectra for quadrupolar nuclei in one dimension in 'real time'. This makes it possible to conceive more complex 2D experiments involving DOR such as multiple quantum DOR (MQDOR) [16–20] and exchange spectroscopy (EXSY) [19–21]. Another technique known as 'satellite transitions acquired in real time by magic-angle-spinning' (STARTMAS) has recently been proposed for the acquisition of isotropic spectra of spin-3/2 nuclei in solids [22,23]. This appealing technique requires both high power pulses to excite the satellite transitions and a very accurately set magic angle, whereas in DOR, only a simple one-pulse excitation is necessary. The principal drawback to DOR NMR is the slow spinning rate because of the large size of the outer rotor. This generally leads to a large number of spinning sidebands which can overlap with other resonances. Although these sidebands in principle contain all the quadrupolar and chemical shift tensor information [24–26], they are more often a hindrance. A method capable of removing all sidebands in DOR is therefore desirable. Progress was made with the discovery that all odd-order sidebands could be suppressed by synchronizing the pulses with the outer rotor phase such that the inner rotor either points upwards or downwards at the moment of excitation [27]. Samoson then showed that by using inversion pulses, it was possible to selectively eliminate particular sideband orders by taking appropriate sums of the results of up to seven different experiments [28,29]. All sidebands in DOR have also been successfully removed using a magic-angle-turning type experiment, although two-dimensional acquisition is necessary [30]. The technique we present here is an extension of Samoson's earlier experiments and in effect is an extension of TOSS to DOR, so as to simultaneously remove all outer-rotor DOR sidebands.

* Corresponding author. Fax: +1 613 562 5170.
E-mail address: dbryce@uottawa.ca (D.L. Bryce).

1090-7807/$ - see front matter © 2011 Elsevier Inc. All rights reserved.
doi:10.1016/j.jmr.2011.05.002

2. Theory

Previous treatments of DOR sidebands have shown that when the inner rotor's spin rate exceeds the breadth of the static line width, then this spin rate can be reasonably approximated as infinite. This approximation has been exploited in the development of the now widely used synchronized experiment to remove half of the sidebands in DOR. Under this approximation, the phase of the time domain NMR signal may be expressed as a sum of four sinusoidal terms [29,31] with an additional "g_n" modulation which is unique to DOR, compared to the MAS case:

$$\varphi(t) = \omega_0 t + \sum_{n=1}^{4} a_n[\sin n(\omega_R t + \gamma) - g_n] \tag{1}$$

where, in the case of one-pulse excitation,

$$g_n = \sin n\gamma, \tag{2}$$

ω_0 is the Larmor angular frequency, ω_R is the outer rotor's spin rate, and γ is the phase of the outer rotor with respect to the magnetic field. The four a_n terms are functions with magnitudes that depend on the different NMR interactions [27]. The first two terms depend on the quadrupolar interaction, chemical shift anisotropy, and dipolar coupling, whereas the two last terms depend only on the second-order quadrupolar interaction. These last terms are much smaller than the first two terms; they then affect the sidebands to a lesser extent.

The phase of the sidebands depends on the rotor orientation as follows:

$$\phi = N\gamma + \sum_{n=1}^{4} a_n g_n \tag{3}$$

In the case of the synchronized DOR experiment [27], g_n is equal to zero for both outer rotor orientations ($\gamma = 0°$ and 180°). The phase of the odd sidebands is then inverted between both orientations and the spectra are free of odd-order sidebands. Using inversion pulses, it is also possible to force g_1 and g_2 to be zero for rotor phases of 90° and 270°. This increase in rotor orientation symmetry removes ¾ of the sidebands [29]. As the DOR sidebands' phases are γ-encoded, unlike in MAS, they can naturally cancel one another through signal averaging [32]. By removing the dependence of g_1 and g_2 on the rotor phase, all contributions from a_1 and a_2 to the sidebands would be removed after considering a large enough set of different γ angles. This concept, alluded to by Samoson and Tegenfeldt [29], is the core foundation for the experiment proposed here.

The effect of inversion pulses on sidebands has proven to be useful in MAS in the case of the TOSS experiment [32]. These pulses invert the phase of the magnetization and can be used to change the initial value of the g_n components of the sidebands. For example, for a delay τ_A followed by a single inversion pulse, the phase components g_n are expressed as follows:

$$g_n(\tau_A) = -2\sin n(\omega_R\tau_A + \gamma) + \sin n\gamma. \tag{4}$$

To completely remove g_1 and g_2, four inversion pulses are necessary. In that case, the g_n terms are expressed as follows:

$$\begin{aligned} g_n = {} & -2\sin n(\gamma + \omega_R\tau_A + \omega_R\tau_B + \omega_R\tau_C + \omega_R\tau_D) + 2\sin n(\gamma \\ & + \omega_R\tau_A + \omega_R\tau_B + \omega_R\tau_C) - 2\sin n(\gamma + \omega_R\tau_A + \omega_R\tau_B) + 2 \\ & \times \sin n(\gamma + \omega_R\tau_A) - 2\sin n(\gamma) \end{aligned} \tag{5}$$

where the delays τ_X (X = A, B, C, D) are ordered alphabetically.

Contrary to the MAS case, the rotor phase dependence of the sidebands needs to be separated to solve the g_1 and g_2 expressions. It is then useful to rearrange the above expressions as follows. The first term, g_1, can be written as such:

$$g_1 = E\sin\gamma + F\cos\gamma \tag{6}$$

where

$$\begin{aligned} E = {} & -\cos(2(\omega_R\tau_A + \omega_R\tau_D)) - 2\cos(\omega_R\tau_A - \omega_R\tau_B - \omega_R\tau_C \\ & + \omega_R\tau_D) + 2\cos(\omega_R\tau_A + 2\omega_R\tau_D) + 4 \\ & \times \sin\left(\frac{\omega_R\tau_C}{2}\right)\sin\left(\omega_R\tau_A - \omega_R\tau_B - \frac{\omega_R\tau_C}{2} + 2\omega_R\tau_D\right), \end{aligned} \tag{7}$$

and

$$\begin{aligned} F = {} & \sin(2(\omega_R\tau_A + \omega_R\tau_D)) + 2\sin(\omega_R\tau_A - \omega_R\tau_B - \omega_R\tau_C \\ & + \omega_R\tau_D) - 2\sin(\omega_R\tau_A + 2\omega_R\tau_D) + 4\sin\left(\frac{\omega_R\tau_C}{2}\right)\cos(\omega_R\tau_A \\ & - \omega_R\tau_B - \frac{\omega_R\tau_C}{2} + 2\omega_R\tau_D)\sin\left(\frac{\omega_R\tau_C}{2}\right) \end{aligned} \tag{8}$$

The second term of interest, g_2, can also be rearranged in this useful fashion:

$$g_2 = G\sin^2\gamma - G\cos^2\gamma + H\sin\gamma\cos\gamma \tag{9}$$

where

$$\begin{aligned} G = {} & 2\sin(2(\omega_R\tau_A - \omega_R\tau_B - 2\omega_R\tau_D)) - 2\sin(2(\omega_R\tau_A - \omega_R\tau_B \\ & + \omega_R\tau_C - 2\omega_R\tau_D)) + 2\sin(2(\omega_R\tau_A - \omega_R\tau_B + \omega_R\tau_C \\ & - \omega_R\tau_D)) - \sin(4(\omega_R\tau_B + \omega_R\tau_D)) - 2\sin(2(\omega_R\tau_A \\ & - 2\omega_R\tau_B - 2\omega_R\tau_D)), \end{aligned} \tag{10}$$

and

$$\begin{aligned} H = {} & -4\cos(2(\omega_R\tau_A - \omega_R\tau_B - 2\omega_R\tau_D)) + 4\cos(2(\omega_R\tau_A \\ & - \omega_R\tau_B + \omega_R\tau_C - 2\omega_R\tau_D)) - 4\cos(2(\omega_R\tau_A - \omega_R\tau_B \\ & + \omega_R\tau_C - \omega_R\tau_D)) - 2\cos(4(\omega_R\tau_B + \omega_R\tau_D)) + 4 \\ & \times \cos(2(\omega_R\tau_A - 2\omega_R\tau_B - 2\omega_R\tau_D)) \end{aligned} \tag{11}$$

If the pulse timings are selected such that E, F, G, and H are zero, then g_1 and g_2 will be zero for all rotor orientations. Since the sideband phase is given by Eq. (3), after summation of sufficient transients corresponding to arbitrary outer rotor phases, all a_1 and a_2 contributions to the sidebands eliminate each other.

A non-zero contribution from a_3 and a_4 remains, which is generally small in comparison with the other contributions; we note that other DOR sideband suppression methods are also not capable of eliminating these terms. The phase terms g_3 and g_4 still have a dependence on the rotor phase angle which is given below:

$$\begin{aligned} g_3 = {} & 3.47\cos^3\gamma + 1.84\cos^2\gamma\sin\gamma - 10.415\cos\gamma\sin^2\gamma \\ & - 0.61\sin^3\gamma \end{aligned} \tag{12}$$

$$\begin{aligned} g_4 = {} & 1.6\cos^4\gamma - 22.59\cos^3\gamma\sin\gamma - 9.59\cos^2\gamma\sin^2\gamma \\ & + 22.59\cos\gamma\sin^3\gamma + 1.6\sin^4\gamma \end{aligned} \tag{13}$$

The value of g_3 then oscillates between 3.53 and −3.53 and g_4 varies from 5.87 to −5.87. To also remove g_3 along with g_1 and g_2 would require six inversion pulses whereas eight inversion pulses are necessary to completely suppress all the sidebands. So many pulses increases the possible effects of pulse imperfections, and more importantly, increases the potential loss of signal due to spin–spin relaxation.

3. Results and discussion

The pulse sequence to remove n = 1 and 2 modulations is depicted in Fig. 1, where the possible pulse delays are given in Table 1. We have referred to this experiment as AMBASSADOR, which stands for Angle Modification Before Acquisition to Suppress

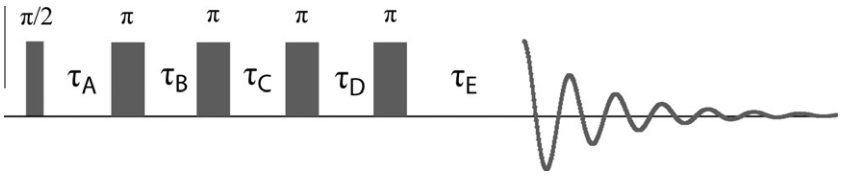

Fig. 1. A schematic representation of the DOR–TOSS sequence.

Table 1
Pulse delays for the DOR–TOSS (AMBASSADOR) experiments.

Sequence	$\omega_R\tau_A$ (°)	$\omega_R\tau_B$ (°)	$\omega_R\tau_C$ (°)	$\omega_R\tau_D$ (°)	$\omega_R\tau_E$ (°)	Total (°)
1	152.61	15.52	236.07	27.88	14.72	446.80
2	44.20	27.88	80.52	15.52	278.68	446.80
3	207.39	80.52	27.88	236.07	81.32	633.18
4	67.98	14.84	209.20	345.16	82.82	720.00
5	67.98	209.20	14.84	150.79	277.19	720.00
6	44.20	123.93	344.48	279.48	14.72	806.81
7	315.80	236.07	15.52	80.52	345.28	993.19
8	292.02	150.79	345.16	209.20	82.83	1080.00
9	292.02	345.16	150.79	14.84	277.19	1080.00
10	152.61	279.48	332.12	123.93	278.68	1166.82
11	207.39	344.48	123.93	332.12	345.28	1353.20
12	315.80	332.12	279.48	344.48	81.32	1353.20

Sidebands Acquired in DOR. In fact, however, the delays that were determined for this sequence are identical to those from the TOSS experiment and therefore the $g_{1,2}$ modulations can be removed in the same way as the modulations in MAS.

A DOR sideband simulation program was written in C to test whether the remaining $n = 3$ and 4 modulations would have an important effect on the spectrum. The free induction decay is calculated according to Eq. (14) and is then Fourier transformed to get the frequency domain spectrum [31]:

$$FID(t) = \frac{1}{8\pi^2}\int_0^{2\pi}\int_0^{\pi}\int_0^{2\pi} \exp(i\varphi(t)) \sin\beta \, d\alpha \, d\beta \, d\gamma \qquad (14)$$

where $\varphi(t)$ is given in Eq. (1). To simulate the DOR–TOSS spectra, the g_n modulations can be taken directly from Eqs. (12) and (13) where the rotor phase at the moment of acquisition needs to be incremented by the duration of the pulse sequence. Simulations performed using the quadrupolar parameters of sodium oxalate ($C_Q = 2.52$ MHz, $\eta = 0.75$) [29,33] and an outer-rotor spin rate of 800 Hz are shown in Fig. 2. Alone, the g_3 and g_4 modulations contribute only to the sidebands of order 3 N and 4 N respectively, although when combined the first and second sidebands are partially reintroduced. According to these idealized simulations, fairly complete sideband suppression can be obtained when we consider only the g_1 and g_2 modulations. To determine whether this is generally the case, simulations were performed by keeping the quadrupolar parameters constant and varying the spin rate, and, in a second instance while keeping the spin rate constant at 1 kHz and systematically incrementing the quadrupolar coupling constant (Fig. 3). It can be seen that the remaining sideband intensity in DOR–TOSS is mainly caused by the g_3 modulations and that at least a five-fold reduction of sideband intensity can be obtained in the slow-spinning or large-C_Q cases.

Of the 12 possible experiments (Table 1), the most appealing sequences are the first two in the table because they last only 1.24 rotor cycles (446.80° of rotation), although the delay for 15.52° of rotor rotation may become too short at high spinning speeds. In such situations, the delay may be increased by a full rotor cycle without affecting the sequence, or, alternatively, sequence 3 which lasts 1.76 rotor cycles and has longer delays may be used. All sequences theoretically remove equal contributions from both g_3 and g_4 and thus the only criteria for selection of the optimal sequence is the desired time between excitation and acquisition. For some of the longer sequences, spin diffusion may become an issue and only a small fraction of the initial magnetization will be refocused. If this is the case, the signal may be entirely lost. As a rule of thumb, to verify if DOR–TOSS will be effective on a given sample, a Hahn echo may be set up with an echo delay equal to half of the total length of the desired DOR–TOSS sequence. If an echo is observed, then this method can be used to suppress sidebands. In Fig. 4, a comparison between the regular DOR spectrum, the synchronized DOR spectrum, and the DOR–TOSS spectrum is shown for sodium oxalate. This test sample was chosen for easy comparison with the prior DOR literature. It may be seen that most of the sidebands are absent or substantially reduced in the DOR–TOSS spectrum whereas the first-order sidebands are more efficiently suppressed with synchronization. DOR–TOSS would then be

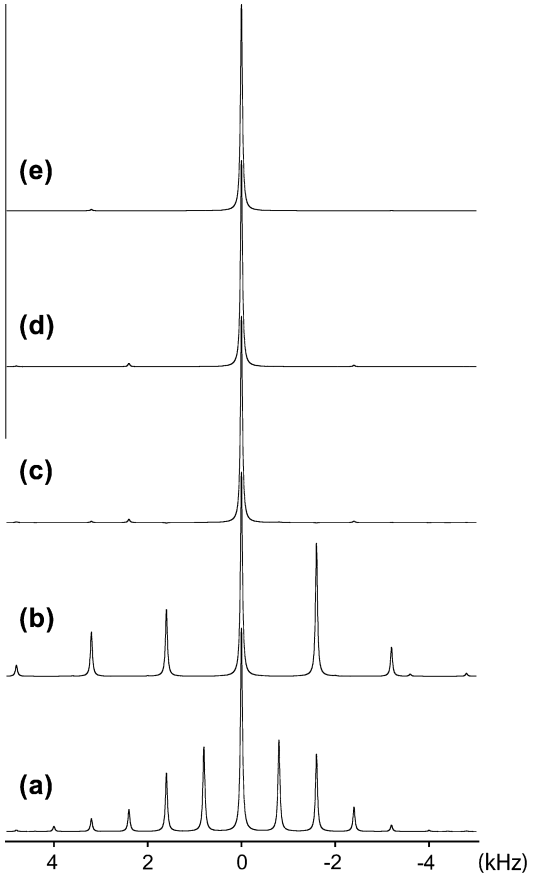

Fig. 2. Numerical simulations of various DOR NMR spectra using an infinite inner rotor spinning frequency, an outer rotor spinning at 800 Hz, and ideal pulses. The parameters used for the simulation are those of sodium oxalate ($C_Q = 2.52$ MHz, $\eta = 0.75$). In (a) the regular DOR spectrum is shown, in (b) the pulses were synchronized with the outer rotor's orientation, in (c) the DOR–TOSS simulation is shown and its contributions arising from the g_3 and g_4 modulations are shown in (d) and (e) respectively. $B_0 = 9.4$ T.

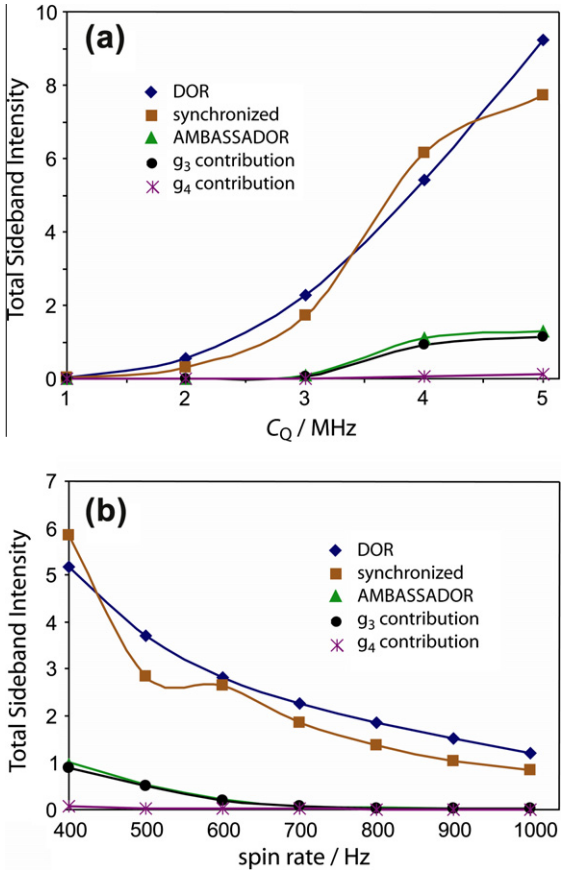

Fig. 3. Numerical simulations of absolute integrated DOR sideband intensities as the quadrupolar coupling constant is varied while keeping a constant outer rotor spinning frequency of 1 kHz (a) and as the spin rate is varied while keeping a constant quadrupolar coupling constant of 2.52 MHz (b). In all simulations the Larmor frequency was set to 105.8 MHz and the asymmetry parameter was 0.75.

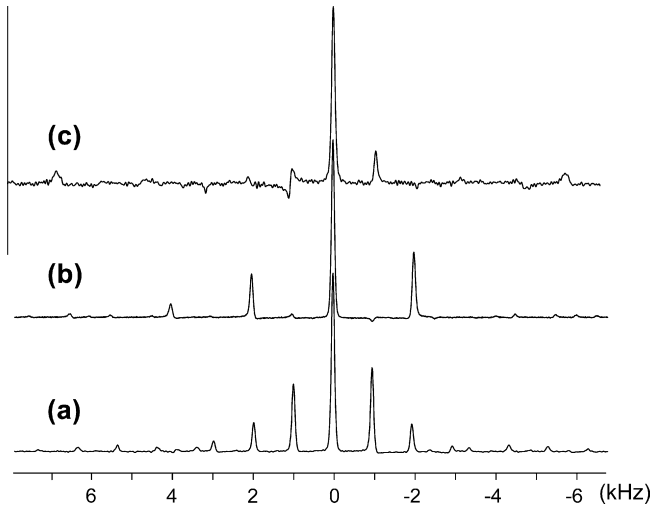

Fig. 4. A comparison of different ^{23}Na DOR NMR experiments on sodium oxalate. (a) The regular, one-pulse DOR spectrum, (b) the synchronized DOR spectrum, and (c) the DOR–TOSS spectrum using experiment 2 from Table 1 while spinning the outer rotor at 1.0 kHz.

advantageous in cases where there is a large number of spinning sidebands, while synchronization is best when there are only a small number of sidebands or when signal-to-noise is an issue.

Naturally, such an experiment may be sensitive to pulse imperfections. In Fig. 5, the DOR–TOSS spectrum is compared to the synchronized experiment [27], Samoson's one- and two-pulse experiments [28,29], as well as a TOSS-9 [34] sequence which should, in theory, remove modulations of orders 1–4. In general, sequences with the fewest pulses appear to better suppress the targeted sidebands and have stronger centreband intensities, although the DOR–TOSS sequence is the shortest sequence which targets all sideband orders. The remaining sidebands in the TOSS-9 and the synchronized experiment are caused by the finite inner rotor rotation which can interfere with the inversion pulses. Our simulations suggest that the loss in intensity is principally caused by pulse imperfections, as the calculated spectra have higher centerband intensities, similar to what is seen in the MAS TOSS case [35].

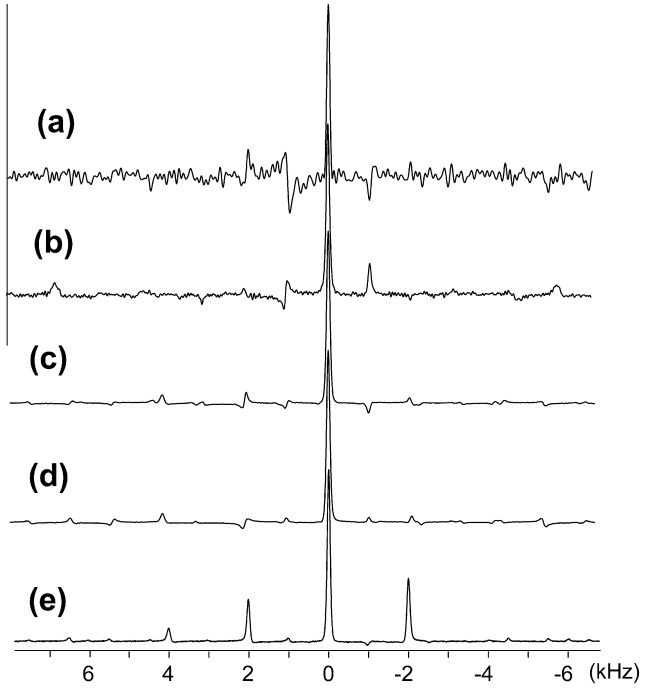

Fig. 5. An experimental comparison of various DOR sideband suppression methods: (a) the TOSS-9 experiment, (b) the DOR–TOSS experiment, (c) Samoson's two-pulse experiment, (d) Samoson's one-pulse experiment, and (e) the synchronized experiment. The relative centreband intensities of the last three experiments in comparison to the DOR–TOSS experiment are 5.42, 6.89 and 18.82, respectively.

To see how the DOR–TOSS experiment performs when multiple sites are present, sodium pyrophosphate was studied, which has four crystallographically and magnetically non-equivalent sodium sites with quadrupolar coupling constants ranging from 2.08 MHz to 3.22 MHz [36]. A comparison of the DOR, synchronized DOR, and DOR–TOSS spectra is given in Fig. 6. The first two spectra contain a large number of sidebands which can render spectral assignment difficult. In the DOR–TOSS spectrum, all sidebands are essentially gone and the four sites can be distinguished although their relative intensities are far from ideal. Since the sites with the smallest quadrupole coupling constants will have a larger proportion of the intensity held in the centreband and will be more effectively refocused by the inversion pulses, they have a larger intensity relative to the higher-C_Q sites. The spectrum is thus dominated by the site having a quadrupolar coupling constant of 2.08 MHz. Two smaller peaks correspond to ^{23}Na sites characterized by quadrupole coupling constants of 2.30 and 2.90 MHz and the last, least intense, peak corresponds to the site characterized by a quadrupole coupling constant of 3.22 MHz. It is therefore a possibility that some high-C_Q sites may be difficult to identify *a priori* when employing DOR–TOSS if diffusion or relaxation is an issue, but this is a drawback also suffered by the other proposed pulsed sideband

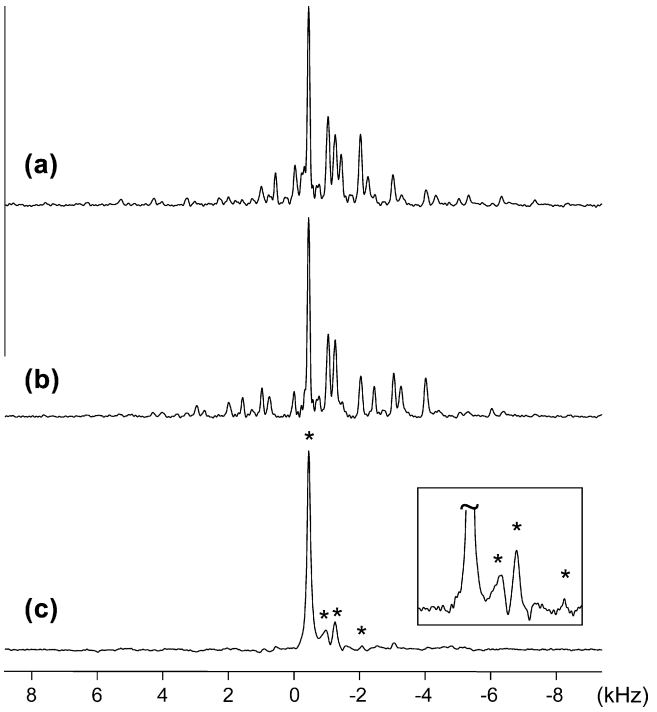

Fig. 6. A comparison of the (a) DOR spectrum, (b) synchronized DOR spectrum, and the (c) DOR–TOSS spectrum of sodium pyrophosphate while spinning the outer rotor at 1.02 kHz. The four centerbands are marked by asterisks.

suppression methods. Importantly, we point out that none of the previous DOR sideband suppression publications have presented any results where multiple sites with a range of C_Q values (e.g., sodium pyrophosphate) are resolved. Finally, we note that the overall signal-to-noise of DOR–TOSS spectra is usually reduced when compared to conventional DOR, and DOR–TOSS spectra therefore typically take more time to acquire, but the end result is a cleaner and easier to interpret DOR spectrum.

4. Conclusions

We have presented an easy to use experiment based on the TOSS experiment for MAS to remove outer rotor sidebands in DOR NMR spectra by removing the rotor phase angle dependence of the sideband evolution. The pulse sequence is simple to implement and only requires that the pulses be measured relatively accurately. This method removes all outer rotor sidebands in DOR without the need to manually sum the results of various experiments using post-processing which can introduce unwanted errors. Unlike the synchronized experiment which removes only half the sidebands [27], DOR–TOSS targets all the sidebands and does not require that the pulses be synchronized with the outer rotor's phase. While the resulting signal is reduced experimentally when compared to idealized simulations and to single-pulse experiments, DOR–TOSS will permit multiple resonances to be distinguished and remove issues arising from peaks overlapping with sidebands. In this context, DOR–TOSS is a useful complement to existing methods.

5. Experimental details

All experiments were conducted on a Bruker Avance III 400 spectrometer operating at 105.8 MHz for ^{23}Na. A Bruker HP WB 73A DOR probe with a 4.3 mm inner rotor and a 14 mm outer rotor capable of achieving outer rotor spinning frequencies of up to approximately 1.1 kHz was used. Typical inner rotor spinning frequencies were 5.5 kHz. The spinning of the inner rotor was monitored by connecting an antenna to the stator of the probe, which was then connected to an oscilloscope. The ^{23}Na NMR spectra for sodium oxalate were acquired using 176 scans whereas 16 and 1024 scans were used for the ^{23}Na DOR and DOR–TOSS spectra of sodium pyrophosphate respectively; 4 s recycle delays and 3.10 μs central transition selective excitation pulses were used in all the experiments. COG11 (7, 6, 7, 6, 7; 0) [37] and COG19 (9, 10, 9, 10, 9, 10, 9, 10, 9, 10; 0) [38] phase cycles were used for the DOR–TOSS and TOSS-9 experiments respectively. Generally, it was observed that a minimum of 32 scans should be used for adequate sideband suppression. This is supported by simulations which show that the sideband intensity and phase has converged once 32 outer-rotor phases are considered (See Fig. S1).

Acknowledgments

F.A.P. is grateful to the Natural Sciences and Engineering Research Council (NSERC) of Canada for a graduate scholarship. D.L.B. thanks NSERC, the Canada Foundation for Innovation, and the Ontario Ministry of Research and Innovation for funding. We thank Dr. Glenn Facey for essential technical support. We are grateful to Dr. Henry Stronks and co-workers at Bruker Biospin for their support of our DOR research program, and to Dr. Alan Wong and Dr. Andreas Brinkmann for helpful advice.

Appendix A. Supplementary data

Supplementary data associated with this article can be found, in the online version, at doi:10.1016/j.jmr.2011.05.002.

References

[1] E.R. Andrew, A. Bradbury, R.G. Eades, Nuclear magnetic resonance spectra from a crystal rotated at high speed, Nature 182 (1958) 1659.
[2] I.J. Lowe, Free induction decays of rotating solids, Phys. Rev. Lett. 2 (1959) 285–287.
[3] A. Pines, M.G. Gibby, J.S. Waugh, Proton-enhanced NMR of dilute spins in solids, J. Chem. Phys. 59 (1973) 569–590.
[4] J. Schaefer, E.O. Stejskal, Carbon-13 nuclear magnetic resonance of polymers spinning at the magic angle, J. Am. Chem. Soc. 98 (1976) 1031–1032.
[5] E.O. Stejskal, J. Schaefer, J.S. Waugh, Magic-angle spinning and polarization transfer in proton-enhanced NMR, J. Magn. Reson. 28 (1977) 105–112.
[6] M.H. Cohen, F. Reif, Quadrupole effects in nuclear magnetic resonance studies of solids, Solid State Phys. 5 (1957) 321–438.
[7] E. Kundla, A. Samoson, E. Lippmaa, High-resolution NMR of quadrupolar nuclei in rotating solids, Chem. Phys. Lett. 83 (1981) 229–232.
[8] A. Samoson, A. Pines, Double rotor for solid-state NMR, Rev. Sci. Instrum. 60 (1989) 3239–3241.
[9] A. Chakraborty, Dynamic balancing in NMR double rotor system, Spectrochim. Acta, Part A 56 (2000) 2725–2727.
[10] A. Samoson, E. Lippmaa, A. Pines, High resolution solid-state N.M.R. Averaging of second-order effects by means of a double-rotor, Mol. Phys. 65 (1988) 1013–1018.
[11] B.F. Chmelka, K.T. Mueller, A. Pines, J. Stebbins, Y. Wu, J.W. Zwanziger, Oxygen-17 NMR in solids by dynamic-angle spinning and double rotation, Nature 339 (1989) 42–43.
[12] Y. Wu, B.Q. Sun, A. Pines, A. Samoson, E. Lippmaa, NMR experiments with a new double rotor, J. Magn. Reson. 89 (1990) 297–309.
[13] L. Frydman, J.S. Harwood, Isotropic spectra of half-integer quadrupolar spins from bidimensional magic-angle spinning NMR, J. Am. Chem. Soc. 117 (1995) 5367–5368.
[14] Z. Gan, Isotropic NMR spectra of half-integer quadrupolar nuclei using satellite transitions and magic-angle spinning, J. Am. Chem. Soc. 122 (2000) 3242–3243.
[15] A. Llor, J. Virlet, Towards high-resolution NMR of more nuclei in solids: sample spinning with time-dependent spinner axis angle, Chem. Phys. Lett. 152 (1988) 248–253.
[16] A. Samoson, Two-dimensional isotropic NMR of quadrupole nuclei in solids, J. Magn. Reson. Ser. A 121 (1996) 209–211.
[17] A. Samoson, T. Anupõld, Synchronized double rotation 2D NMR, Solid State Nucl. Magn. Reson. 15 (2000) 217–225.
[18] I. Hung, A. Wong, A.P. Howes, T. Anupõld, A. Samoson, M.E. Smith, D. Holland, S.P. Brown, R. Dupree, Separation of isotropic chemical and second-order quadrupolar shifts by multiple-quantum double rotation NMR, J. Magn. Reson. 197 (2009) 229–236.

[19] I. Hung, A.P. Howes, B.G. Parkinson, T. Anupõld, A. Samoson, S.P. Brown, P.F. Harrison, D. Holland, R. Dupree, Determination of the bond-angle distribution in vitreous B_2O_3 by ^{11}B double rotation (DOR) NMR spectroscopy, J. Solid State Chem. 182 (2009) 2402–2408.
[20] A.P.M. Kentgens, E.R.H. van Eck, T.G. Ajithkumar, T. Anupõld, J. Past, A. Reinhold, A. Samoson, New opportunities for double rotation NMR of half-integer quadrupolar nuclei, J. Magn. Reson. 178 (2006) 212–219.
[21] I. Hung, A.P. Howes, T. Anupõld, A. Samoson, D. Massiot, M.E. Smith, S.P. Brown, R. Dupree, ^{27}Al double rotation two-dimensional spin diffusion NMR: complete unambiguous assignment of aluminium sites in $9Al_2O_3{\cdot}2B_2O_3$, Chem. Phys. Lett. 432 (2006) 152–156.
[22] M.J. Thrippleton, T.J. Ball, S. Steuernagel, S.E. Ashbrook, S. Wimperis, STARTMAS: A MAS-based method for acquiring isotropic NMR spectra of spin $I = 3/2$ nuclei in real time, Chem. Phys. Lett. 431 (2006) 390–396.
[23] M.J. Thrippleton, T.J. Ball, S. Wimperis, Satellite transitions acquired in real time by magic angle spinning (STARTMAS): "Ultrafast" high-resolution MAS NMR spectroscopy of spin $I = 3/2$ nuclei, J. Chem. Phys. 128 (2008) 034507.
[24] E. Cochon, J.P. Amoureux, Sideband analysis in DOR NMR spectra I. "Infinite" inner-rotor speed, Solid State Nucl. Magn. Reson. 2 (1993) 205–222.
[25] J.P. Amoureux, E. Cochon, Sideband analysis in DOR NMR spectra II. Real finite inner-rotor speed, Solid State Nucl. Magn. Reson. 2 (1993) 223–234.
[26] I. Hung, A. Wong, A.P. Howes, T. Anupõld, J. Past, A. Samoson, X. Mo, G. Wu, M.E. Smith, S.P. Brown, R. Dupree, Determination of NMR interaction parameters from double rotation NMR, J. Magn. Reson. 188 (2007) 246–259.
[27] A. Samoson, E. Lippmaa, Synchronized double-rotation NMR spectroscopy, J. Magn. Reson. 84 (1989) 410–416.
[28] A. Samoson, Approximate approach to DOR sideband suppression, Chem. Phys. Lett. 214 (1993) 456–458.
[29] A. Samoson, J. Tegenfeldt, Suppression of DOR sidebands, J. Magn. Reson., Ser. A 110 (1994) 238–244.
[30] D. Kuwahara, T. Nakai, Spinning-sideband suppression in DOR NMR spectra using a magic-angle-turning technique, Chem. Phys. Lett. 260 (1996) 249–252.
[31] B.Q. Sun, J.H. Baltisberger, Y. Wu, A. Samoson, A. Pines, Sidebands in dynamic angle spinning (DAS) and double rotation (DOR) NMR, Solid State Nucl. Magn. Reson. 1 (1992) 267–295.
[32] W.T. Dixon, Spinning-sideband-free and spinning-sideband-only NMR spectra in spinning samples, J. Chem. Phys. 77 (1982) 1800–1809.
[33] A. Samoson, P. Sarv, J.P. van Braam Houckgeest, B. Kraushaar-Czarnetzki, Chemical shift anisotropy of ^{27}Al in $AlPO_4$–21, Appl. Magn. Reson. 4 (1993) 171–178.
[34] O.N. Antzutkin, Z. Song, X. Feng, M.H. Levitt, Suppression of sidebands in magic-angle-spinning nuclear magnetic resonance: General principles and analytical solutions, J. Chem. Phys. 100 (1994) 130–140.
[35] E.T. Olejniczak, S. Vega, R.G. Griffin, Multiple pulse NMR in rotating solids, J. Chem. Phys. 81 (1984) 4804–4817.
[36] G. Engelhardt, A.P.M. Kentgens, H. Koller, A. Samoson, Strategies for extracting NMR parameters from ^{23}Na MAS, DOR and MQMAS spectra. A case study for $Na_4P_2O_7$, Solid State Nucl. Magn. Reson. 15 (1999) 171–180.
[37] A. Jerschow, R. Kumar, Calculation of coherence pathway selection and cogwheel cycles, J. Magn. Reson. 160 (2003) 59–64.
[38] N. Ivchenko, C.E. Hughes, M.H. Levitt, Application of cogwheel phase cycling to sideband manipulation experiments in solid-state NMR, J. Magn. Reson. 164 (2003) 286–293.